Carbohydrate Polymers 117 (2015) 980–987

Contents lists available at ScienceDirect

Carbohydrate Polymers

journal homepage: www.elsevier.com/locate/carbpol

A comparative study of the neutral and acidic polysaccharides from *Allium macrostemon* Bunge

Zhanjun Zhang[a,b], Fuhua Wang[c], Mingchun Wang[a], Liping Ma[a], Hong Ye[a], Xiaoxiong Zeng[a,*]

[a] College of Food Science and Technology, Nanjing Agricultural University, Nanjing 210095, PR China
[b] College of Biological and Chemical Engineering, Yangzhou Vocational University, Yangzhou 225009, PR China
[c] Department of Chemical Engineering, Yangzhou Polytechnic Institute, Yangzhou 225127, PR China

ARTICLE INFO

Article history:
Received 4 June 2014
Received in revised form
14 September 2014
Accepted 13 October 2014
Available online 23 October 2014

Keywords:
Allium macrostemon Bunge
Polysaccharides
Characterization
Antitumor activity

ABSTRACT

Neutral and acidic polysaccharides, named AMP40N and AMP40S respectively, were isolated and purified from the dried bulbs of *Allium macrostemon* Bunge. Both of them showed a single and symmetrically sharp peak, indicating they were homogeneous polysaccharides. Molecular weights of AMP40N and AMP40S were determined to be 18.2 and 105.1 kDa, respectively. AMP40N was composed of arabinose and glucose, while AMP40S was composed of rhamnose, arabinose, glucose and galactose and a certain amount of uronic acid. FT-IR, periodic acid oxidation, Smith degradation, methylation and GC–MS analysis revealed that non-reducing terminal and →2,6)-Glc-(1→ existed in AMP40N and AMP40S. The glycosidic linkage of arabinose in AMP40N was →2)-Ara-(1→, whereas it was Ara-(1→ in AMP40S. AMP40S had (1→2)-linked L-rhamnose residue. Both AMP40N and AMP40S exhibited strong anti-tumor potential against human gastric carcinoma cells BGC-823, in particular, AMP40S presented significantly higher inhibitory rate of 85.94% than AMP40N of 52.63%.

1. Introduction

Recently, increasing attention has been paid on polysaccharides as an important class of bioactive natural products, due to their potential biological activities such as anti-tumor (Bai et al., 2012; Xin et al., 2012), anti-oxidant (Wang, Sun, Zhang, Chen, & Liu, 2012; Zhang, Li, Xia, & Lin, 2013), anti-coagulant (Cai, Xie, Chen, & Zhang, 2013; Lu, Mo, Guo, & Zhang, 2012) and immunomodulatory activities (Sun, Wang, & Zhou, 2012; Wong, Lai, & Cheung, 2011). It is well known that the bioactivities of polysaccharides are most closely related to their chemical composition, configuration, molecular weight, degree of branching and chain conformation (Huang, Jin, Zhang, Cheung, & Kennedy, 2007; Zhang, Gu, et al., 2010). However, the overall complexity of polysaccharides has hindered the elucidation of actual structure-function relationships because there has not been an ideal method available for assessing the full structures of polysaccharides up to now (Tian, Zhao, Guo, & Yang, 2011). It has been reported that acidic polysaccharides are likely to be more bioactive than neutral polysaccharides (Xie, Schepetkin, & Quinn, 2007), which may be due to the fact that the acidic groups in acidic polysaccharides can form associations with the target biomolecules such as proteins in the hosts through electronic interactions (Wang et al., 2011). Therefore, a comparative study of the chemical structure, chain conformation and bioactivities of neutral and acidic polysaccharides is helpful for better elucidation of the relationship between structure and biological activity of polysaccharides.

Allium macrostemon Bunge, as a well-known traditional Chinese medicine and an edible plant named 'Xiao-gensuan', is a bulb of liliaceous plant that is cultivated in north and northeast China (Peng, Wang, & Yao, 1993). To elucidate the possible pharmacological mechanisms of *A. macrostemon* Bunge, research has been carried out on the low molecular compounds (Kuroda, Mimaki, Kameyama, Sashida, & Nikaido, 1995; Peng et al., 1993; Peng, Yao, Tezuka, & Kikuchi, 1996; Xie et al., 2008). In our previous report, the fraction obtained by 40% ethanol precipitation of crude polysaccharides from *A. macrostemon* Bunge (AMP40) exhibited relatively higher anti-oxidant and anti-tumor activities *in vitro* than the other two fractions (Zhang, Wang, Wang, Ma, & Zeng, 2012). Therefore, the objectives of the present study were to purify the crude AMP40 by anion-exchange and gel filtration chromatography, to characterize the purified fractions by Fourier-infrared spectroscopy (FT-IR), high performance liquid chromatography (HPLC), nuclear magnetic

* Corresponding author. Fax: +86 25 84396791.
E-mail address: zengxx@njau.edu.cn (X. Zeng).

http://dx.doi.org/10.1016/j.carbpol.2014.10.019
0144-8617/

resonance (NMR) spectrometry, gas chromatography (GC), periodic acid oxidation, Smith degradation and methylation combined with GC–mass spectrometry (GC–MS), and to investigate the antitumor activities *in vitro* of purified fractions by determining their inhibitory rates against human gastric cancer BGC-823 cells.

2. Materials and methods

2.1. Materials

The dried bulbs of *A. macrostemon* Bunge were obtained from Anhui Huilong Co., Ltd (Hefei, China). Arabinose, rhamnose, fucose, xylose, galactose, glucose, mannose, dimethyl sulfoxide (DMSO), 3-(4,5-dimethylthiazol-2-yl)-2,5-diphenyl tetrazolium bromide (MTT), DEAE-52 cellulose and Sephadex G-100 were purchased from Sigma Chemical Co. (St. Louis, MO, USA). Human gastric cancer BGC-823 cell line was obtained from the Cell Bank of Shanghai Institute of Cell Biology (Shanghai, China). RPMI-1640 media was purchased from Gibco/Invitrogen (Grand Island, NY, USA). All other chemicals used in the experiment were of analytical grade.

2.2. Preparation and purification of polysaccharides

2.2.1. Preparation of AMP40

The preparation of AMP40 was carried out according to our method reported (Zhang et al., 2012). Briefly, the pretreated bulbs were extracted with water (the ratio of water to raw material 12 mL/g) three times at 87 °C for 100 min. After centrifugation (4500*g*, 10 min), the supernatants were concentrated under vacuum and treated with alcohol to a concentration of 40% (v/v) for precipitation at 20 °C overnight. The precipitate was dissolved in water and dialyzed against distilled water (exclusion limit 8–14 kDa). The non-dialyzable portion was frozen at −20 °C and freeze-dried to afford AMP40.

2.2.2. Purification of AMP40

AMP40 was purified by column chromatography. Firstly, AMP40 (200 mg) was dissolved in 5 mL of distilled water and applied to a column (2.6 × 30 cm) of DEAE-cellulose 52. The column was pre-equilibrated with water and eluted successively with deionized water, 0.1, 0.3 and 0.5 M NaCl solutions at a flow rate of 1.0 mL/min. Fractions (10 mL/tube) were collected by a fraction collector and analyzed for the carbohydrate content by the phenol-sulfuric acid assay (Dubois, Gilles, Hamilton, Rebers, & Smith, 1956). The resulting fractions were further purified by a column of Sephadex G-100 (1.5 × 70 cm), eluting with 0.1 M NaCl solution at a flow rate of 0.05 mL/min. Fractions were analyzed for the carbohydrate content, collected, concentrated, dialyzed against distilled water and lyophilized, affording the neutral and acidic polysaccharide fractions of AMP40N and AMP40S.

2.3. Chemical and structural analysis

2.3.1. Determination of contents of carbohydrate, protein, uronic acid and sulfuric radical

The content of carbohydrate was determined by the phenol-sulfuric acid method (Dubois et al., 1956). Protein concentration was determined using the Bradford assay method (Bradford, 1976), and bovine serum albumin (BSA) was used as a standard to construct the calibration curve. The uronic acid content was measured by a modified hydroxydiphenyl assay (Blumenkrantz & Asboe-Hansen, 1973) with D-glucuronic acid as the standard. The content of sulfuric radical was determined according to the method reported (Dodgson & Price, 1962).

2.3.2. Monosaccharide composition analysis

The monosaccharide composition was analyzed according to the method reported (Qiao et al., 2010) with minor changes. Briefly, polysaccharides sample (5 mg) was hydrolyzed with 2 mL of 2 M trifluoroacetic acid (TFA) at 120 °C for 2 h. The hydrolyzates were repeatedly co-distilled with methanol to dryness and converted into their corresponding aldonitrile acetates by the addition of hydroxylammonium chloride (10 mg), inositol (5 mg), pyridine (0.6 mL) and acetic anhydride (1.0 mL). The aldonitrile acetate derivatives of standard monosaccharides were prepared in the same way. Then, all the derivatives were analyzed by GC (GC 6890N, Agilent) equipped with a flame ionization detector (FID) and an HP-5 fused silica capillary column (30 m × 0.32 mm × 0.25 mm). The operation conditions of GC were as following: flow rates of N_2, H_2 and air were 25, 30 and 400 mL/min, respectively; the temperature of injector and detector were set at 250 and 280 °C, respectively; the initial column temperature was held at 120 °C for 3 min, then programed at a rate of 3 °C/min to 210 °C and held for 4 min.

2.3.3. Molecular weight determination

Homogeneity and the molecular weights of fractions were analyzed according to the method reported (Zhang, Gu, et al., 2010) with slight modification. A HPLC apparatus (Agilent 1100) equipped with a TSK-Gel G3000 SW_{XL} column (7.8 mm × 300 mm, Tosoh Corp., Tokyo, Japan) and a refractive index detector (RID). Sample (20 μL) was injected in and eluted with 0.1 M Na_2SO_4 (dissolved in 0.01 M phosphate buffer of pH 6.8) at a flow rate of 0.6 mL/min. The temperature of the column and detector was set at 25 °C. The calibration curve for molecular weight determination was made using a series of Pullulan P-800, P-400, P-200, P-100, P-20, P-10 and P-5 (Shodex standard P-82, Showadenko, Tokyo, Japan) as standards, following the method described by Alsop and Vlachogiannis (1982).

2.3.4. FT-IR analysis

The FT-IR spectra of polysaccharides were recorded with a Nicolet 200 FT-IR spectrometer (Thermo Fisher Scientific Inc., Waltham, MA, USA) in the range of 4000–500 cm^{-1} by the potassium bromide (KBr) pellet method (Kumar, Joo, Choi, Koo, & Chang, 2004).

2.3.5. Periodic acid oxidation, Smith degradation and GC analysis

Assay of periodic acid oxidation, Smith degradation and GC were performed by using the method reported by Qiao et al. (2010) with slight modification. Briefly, sodium metaperiodate ($NaIO_4$, 0.015 M) and sodium iodate ($NaIO_3$, 0.015 M) were mixed at different ratios and the mixed solution was detected on spectrophotometer at 223 nm, affording a standard curve of $NaIO_4$. Polysaccharide sample (25 mg) was dissolved in 25 ml 15 mmol/L of $NaIO_4$. The solution was kept in the dark at 4 °C with interval stirring, 0.1 mL aliquots were withdrawn at 12 h intervals, diluted to 25 mL with distilled water, and absorbance at 223 nm of dilution was detected. When absorbance did not descend, the reaction was complete and the excess of $NaIO_4$ was decomposed with ethylene glycol (1.0 mL). Consumption of $NaIO_4$ was calculated according to the $NaIO_4$ standard curve. Yield of formic acid (HCOOH) produced was determined by titration and calculated according to the consumption of NaOH. The reaction mixture was reduced with sodium borohydride ($NaBH_4$, 50 mg) for 20 h at 25 °C, and then was adjusted to pH 5.5–7.0 with acetic acid (0.1 M). The reaction solution was dialyzed, freeze-dried, hydrolyzed, derivatized and analyzed by GC as mentioned above. As references, standard monosaccharides, glycerol and erythritol were derivatized and analyzed.

2.3.6. Methylation and GC–MS analysis

Polysaccharide sample was methylated three times using the method of Ciucanu and Kerek (1984) with slight modifications. The completeness of methylation was confirmed by the disappearance

of the O—H absorption band in FT-IR spectrum in 3400 cm^{-1}. The completely methylated product was hydrolyzed with TFA, reduced with $NaBH_4$ and derivatized with pyridine-acetic anhydride. The derivatized product was analyzed on a Varian CP-3800 gas chromatograph coupled with a Saturn 2000 ion trap mass spectrometer (Walnut Creek, CA, USA). A DB-5MS fused silica capillary column (30 m × 0.25 mm × 0.25 μm, J & W Scientific, Folsom, CA, USA) was used with He as a carrier gas, and temperature programed from 80 °C (1 min) up to 210 °C (1 min) at 8 °C/min then up to 260 °C (1 min) at 20 °C/min.

2.3.7. NMR analysis

The polysaccharides samples were dried in a vacuum over P_2O_5 for several days, and then exchanged with deuterium by freeze-drying with deuterium oxide (D_2O) three times (Li, Fan, & Ding, 2011). The deuterium-exchanged polysaccharides samples were put in NMR tubes and dissolved with D_2O. NMR spectra were recorded on a Bruker DRX-600 spectrometer. Tetramethylsilane (TMS) was used as a chemical shift reference.

2.3.8. Helix-coil transition assay

Helix-coil transition assay was performed by using Congo red dye according to the method reported (Qiao et al., 2010) with slight modifications. The solutions of AMP40N and AMP40S (5 mg/mL) were mixed with 80 μM Congo red dye solution. NaOH solution (1.0 M) was added to make the alkali concentration in the mixed solution being changed from 0.0–0.5 M. After reaction for 3 h, the visible spectra were scanned from 400 to 800 nm at room temperature with a Shimadzu UV-2450 spectrophotometer (Shimadzu, Kyoto, Japan) and the maximum absorption wavelength was recorded.

2.4. Assay of inhibitory activity in vitro on BGC-823 cell proliferation

Inhibitory activities *in vitro* of AMP40N and AMP40S were evaluated according to the MTT-based colorimetric method (Mosmann, 1983) with slight modifications. Briefly, BGC-823 cells in the RPMI-1640 medium supplemented with fetal bovine serum (10%), penicillin (100 U/mL) and streptomycin (100 μg/mL) were seeded into 96-well plate (100 μL/well) at a density of 1×10^5 cells/mL. The plate was incubated in 5% CO_2 atmosphere at 37 °C for 24 h. Then, fresh medium (100 μL/well, control group) and different concentration polysaccharide sample (100 μL/well, at a final concentration of 25, 50, 100, 200 and 400 mg/L) were added and further incubation was carried out at 37 °C for 24, 48 and 72 h, respectively. After incubation, MTT solution (5 mg/mL, 10 μL/well) was added to each well, and the plate was incubated for an additional 4 h at 37 °C and the culture medium was removed. Finally, 100 μL of DMSO were added to each well. The absorbance of each well at 550 nm was measured by an ELISA plate reader (TECAN Infinite F200, Switzerland). The inhibition rate was calculated according to the formula below:

$$\text{Inhibition rate}\,(\%) = (1 - A_1/A_2) \times 100\%$$

where A_1 and A_2 are the absorbances of experimental group and blank control group, respectively.

2.5. Statistical analysis

All data presented are means ± SD of triplicates. The Bonferroni test and one-way analysis of variance (ANOVA) were used for multiple comparisons by the SPSS 19.0 software package (Chicago, IL, USA). Difference was considered to be statistically significant if $P < 0.05$.

Table 1
Preliminary characterization of polysaccharide from *Allium macrostemon* Bunge.

Item	AMP40	AMP40N	AMP40S
Carbohydrate (%)	69.93 ± 2.19	80.34 ± 2.27	68.49 ± 1.74
Protein (%)	0.238 ± 0.04	–[a]	–
Uronic acid (%)	12.56 ± 0.73	2.06 ± 0.52	30.22 ± 1.14
Sulfuric radical (%)	0.56 ± 0.06	0.54 ± 0.08	0.91 ± 0.11

[a] Not detected.

3. Results and discussion

3.1. Purification and characterization of polysaccharides

3.1.1. Purification of AMP40

AMP40 was prepared from *A. macrostemon* Bunge by water extraction with a yield of 3.28 ± 0.31%. The resulting AMP40 was firstly separated through an anion-exchange chromatography of DEAE-cellulose 52, affording two independent elution peaks. The two fractions were collected, concentrated and further purified by gel filtration chromatography of Sephadex G-100, respectively. As results, each fraction generated one single elution peak, named AMP40N (a neutral polysaccharide fraction, 49.72 ± 0.18%) and AMP40S (an acidic polysaccharide fraction, 11.80 ± 0.21%), respectively.

3.1.2. Characterization of polysaccharides

The contents of carbohydrate, protein, uronic acid and sulfate in AMP40, AMP40N and AMP40S were measured. The results showed that AMP40S was quite different from AMP40N, as AMP40S had much higher uronic acid content and relatively lower total sugar content (Table 1).

GC chromatograms of standard monosaccharides, AMP40N and AMP40S are shown in Fig. 1. GC analysis showed that AMP40N was composed of arabinose and glucose in a molar ratio of 1.00:5.03 (Fig. 1B). AMP40S was composed of rhamnose, arabinose, glucose and galactose in a molar ratio of 1.41:2.34:1.62:1.00 (Fig. 1C). The results indicated that monosaccharide composition of AMP40S was more complex than that of AMP40N.

The molecular weights of AMP40N and AMP40S were determined by HPLC with size exclusion column. As shown in Fig. 2A and B, both of them showed a single, symmetrically sharp peak, indicating that both the AMP40N and AMP40S were homogeneous polysaccharides. According to the calibration curve of the elution times of standards, the molecular weights of AMP40N and AMP40S were estimated to be 18.2 and 105.1 kDa, respectively.

FT-IR analytical results indicated that the two samples showed typical peaks of polysaccharides. As shown in Fig. 3, the characteristic absorptions of polysaccharides, a broadly-stretched intense peak at 3300–3500 cm^{-1} for O—H stretching vibrations, were observed. The absorptions around 2920–2940 cm^{-1}, attributed to the asymmetrical stretching vibration of CH_2-group (Zhang, He, et al., 2010), were also observed. In Fig. 3A, the absorption band at 1652 cm^{-1} as assigned to OH deformation vibration (Zhu et al., 2011). The absorption peak at 817 cm^{-1} suggested the presence of sulfate group (Brasch, Chang, Chuah, & Melton, 1981). In Fig. 3B, the band near 1741 cm^{-1} resembled the stretching vibration of C=O in the protonated carboxylic acid, which is present in uronic acid (Wang et al., 2011). The results are in coincidence with the fact that AMP40S had relatively higher uronic acid content (Table 1). Furthermore, the characteristic absorption bands at 833 and 894 cm^{-1} indicated that AMP40S contained both α- and β-glycosidic linkages (Zhang, Gu, et al., 2010).

The periodate oxidation experiment showed that 2.24 and 1.26 mol of $NaIO_4$ were consumed and 0.15 and 0.33 mol of formic acid were produced per mole sugar residue for AMP40N

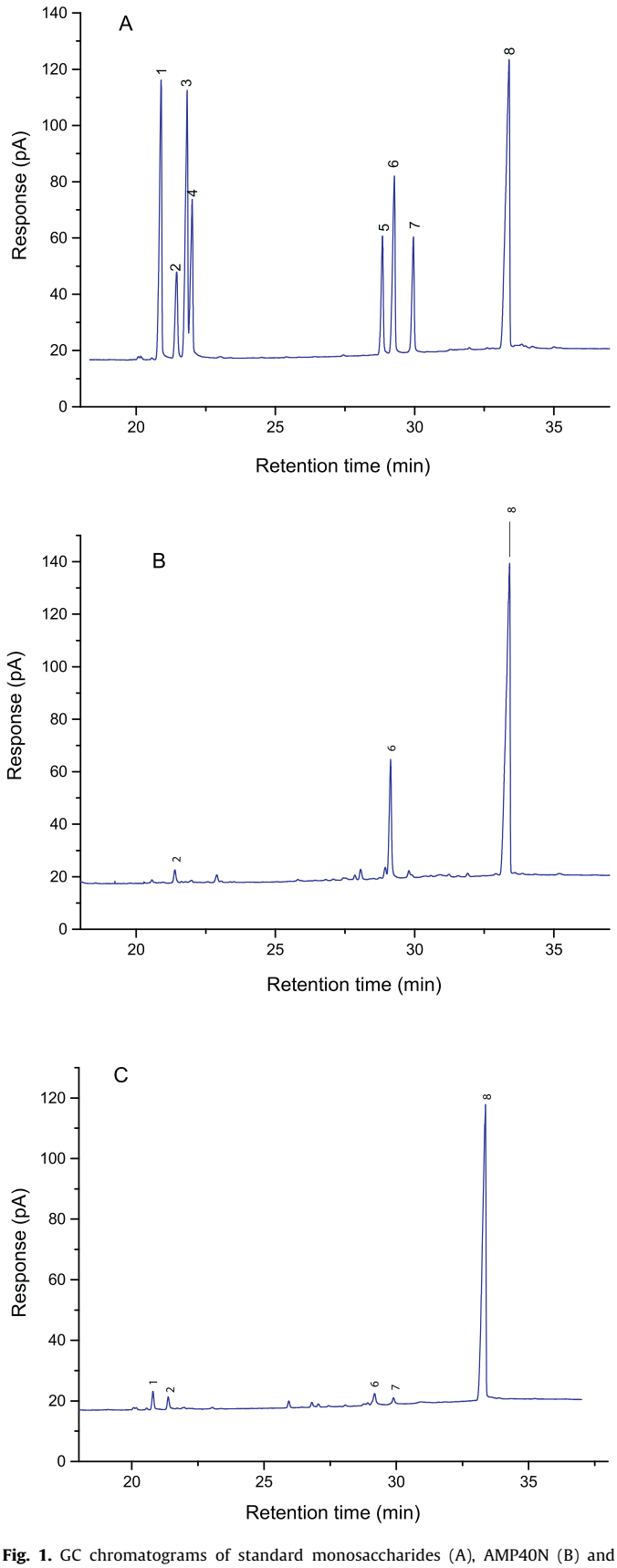

Fig. 1. GC chromatograms of standard monosaccharides (A), AMP40N (B) and AMP40S (C). 1, rhamnose; 2, arabinose; 3, fucose; 4, xylose; 5, mannose; 6, glucose; 7, galactose; 8, inositol.

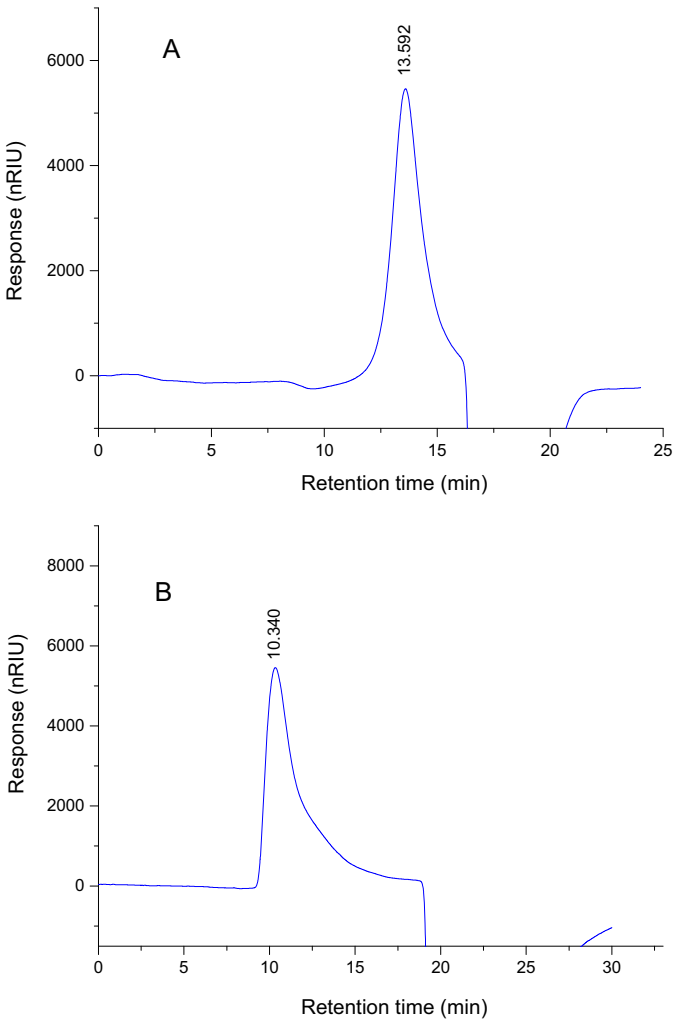

Fig. 2. HPGPC elution profiles of AMP40N (A) and AMP40S (B).

and AMP40S, respectively. These could be inferred that the non-reducing terminal residues or 1→6 linked glycosidic bonds were existed in AMP40N and AMP40S. For each the consumption of $NaIO_4$ was more than double the HCOOH production, meaning that 1→2 or 1→2,6 or 1→4 or 1→4,6 linked glycosidic bonds existed in both AMP40N and AMP40S.

The periodate-oxidized products of polysaccharide were hydrolyzed and examined by GC. As shown in Fig. 4B, the predominant presence of glycerol revealed that the linkages of backbone were 1→2 or 1→6 or 1→2,6 glycosidic linkages that could be oxidized to produce glycerol. The absence of erythritol indicated that the 1→4 and 1→4,6 glycosidic linkage were not present in the backbone of AMP40N. It was thus deduced that AMP40N was linked mainly by 1→2 or 1→6 or 1→2,6 glycosidic bonds. The GC chromatogram of AMP40S after periodic acid oxidation and Smith degradation was presented in Fig. 4C. According to the presence of glycerin, it is deduced that the linkages of main chain could be 1→2 or 1→6 or 1→2,6 glycosidic linkages. The presence of erythritol indicated that the 1→4 or 1→4, 6 glycosidic linkages were present in the backbone of AMP40S. Rhamnose, Arabinose and Glucose were produced in the Smith degradation of AMP40S, which means that some glycosyls were not oxidized in periodic acid oxidation. Galactose was absent, it should be inferred that galactose was in linkages that could be oxidized, namely 1→ or 1→2 or 1→6 or 1→2,6 or 1→4 or 1→4,6 linked glycosidic bonds (Zha, Luo, Luo, & Jiang, 2007).

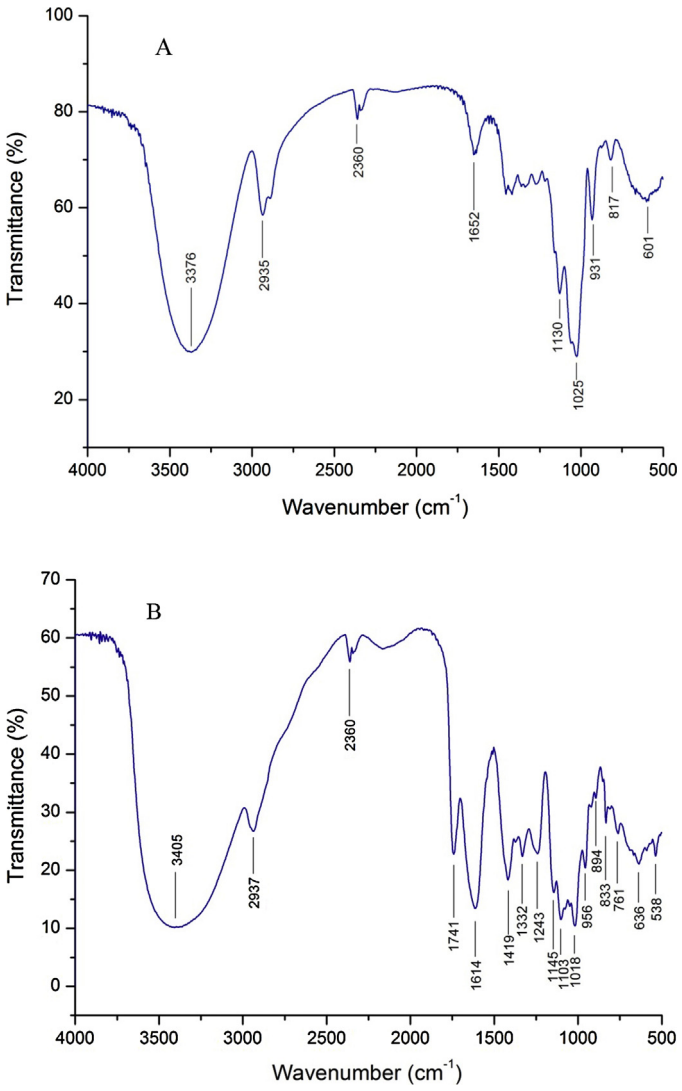

Fig. 3. FT-IR spectra of AMP40N (A) and AMP40S (B).

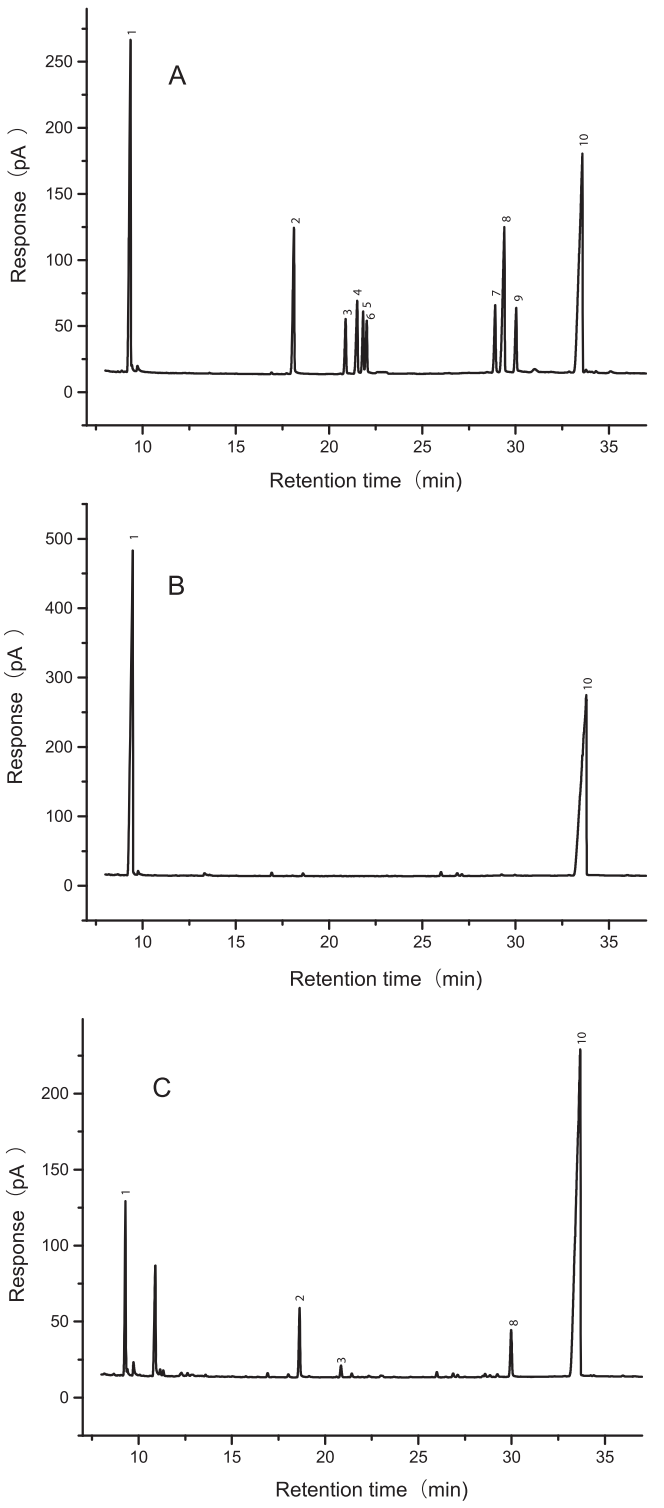

Fig. 4. GC chromatograms of derivatives from standard monosaccharides (A), AMP40N (B) and AMP40S (C) after periodic acid oxidation and Smith degradation. 1, glycerol; 2, erythritol; 3, rhamnose; 4, arabinose; 5, fucose; 6, xylose; 7, mannose; 8, glucose; 9, galactose; 10, inositol.

To determine further the linkage of monosaccharides in AMP40N and AMP40S, they were methylated, hydrolyzed and converted into their corresponding alditol acetates for GC–MS analysis. The results of the methylation analysis of AMP40N and AMP40S are displayed in Table 2. Non-reducing terminal and →2,6)-Glc-(1→ were detected in both AMP40N and AMP40S. The glycosidic linkages of arabinose in AMP40N and AMP40S were significantly different, AMP40N had →2)-Ara-(1→ linkage, whereas AMP40S had Ara-(1→linkage. A small amount of 1,2,5-tri-*O*-acetyl-3,4-di-*O*-methyl-L-rhamnitol, which originated from the (1→2)-linked L-rhamnose residue, was found in AMP40S. Furthermore, the relative molar percentage of each linkage was different between AMP40N and AMP40S.

The structural features of AMP40N and AMP40S were further elucidated by NMR spectral analysis. In the ^{1}H NMR spectrum of AMP40N (Fig. 5A), no signals were observed in the region of δ5–6 ppm, indicating that sugar residues and sugar rings of AMP40N were β-configurations and pyranose rings. A group of signals at δ3.5–4.2 ppm were produced by C-2—C-6 protons. The ^{13}C NMR spectra of AMP40N (Fig. 5B) showed the signals were centralized around δ103 ppm, indicating there was β anomeric configuration of monosaccharide residues existing. The presence of C-1 signal confirmed that all monomers should be pyranose ring, as furanose ring signals should be around δ107–109 ppm (Zhu et al., 2011). In the ^{1}H NMR spectrum of AMP40S (Fig. 5 C), the signal at δ5.15 ppm indicated the existence of α-configuration in AMP40S. The ^{13}C NMR spectrum of AMP40S (Fig. 5D) showed the anomeric peaks were centralized between δ96.20 and δ104.45 ppm, indicating that there were α- and β-anomeric configuration existing in

Table 2
Results of methylation analysis of AMP40N and AMP40S.

Methylation product	Mass fragments (*m/z*)	Linkage type			
		AMP40N	Molar ratios %	AMP40S	Molar ratios %
2,3,4,6-Me_4-Glc	43,87,129,161,205,263,291	Glc-(1→	8.1	Glc-(1→	13.8
3,5-Me_2-Ara	43,87,129,161,221,263,291	→2)-Ara-(1→	6.8	n.d.	–
2,3,4-Me_3-Glc	43,87,111,129,161,189,259,291	→6)-Glc-(1→	36.3	n.d.	–
3,4,6-Me_3-Glc	43,87,111,129,161,189,217,259,291	→2)-Glc-(1→	29.7	n.d.	–
3,4-Me_2-Glc	43,87,129,159,189,217,277,319	→2,6)-Glc-(1→	19.1	→2,6)-Glc-(1→	14.1
2,3,4,-Me_3-Rha	43,103,135,195,281	n.d.[a]	–	Rha-(1→	10.1
2,3,5-Me_3-Ara	43,103,159,162	n.d.	–	Ara-(1→	34.3
3,4-Me_2-Rha	43,99,127,159,209,227,281	n.d.	–	→2)-Rha-(1→	11.5
2,3,4-Me_3-Gal	43,87,129,161,189,259,291	n.d.	–	→6)-Gal-(1→	16.2

[a] Not detected.

AMP40S. Signals δ175.17 and 170.90 ppmwere observed, indicating the presence of uronic acid in AMP40S. The results are agreement with those of FT-IR.

The triple helix structure of the polysaccharides can be evaluated from the trend in the absorption wavelength maximum (Ogawa, Wanatabe, Tsurugi, & Ono, 1972). Change trends in absorption wavelength maximum of a mixture of Congo red and two polysaccharides at different concentrations of alkali were investigated (data not shown). It revealed that the maximum absorption wavelength of AMP40S increased firstly then decreased with increasing concentrations of alkali, while that of AMP40N decreased gradually with the increasing of NaOH concentration. The results indicated that AMP40S possessed the triple helical structure and AMP40N did not have the structure of triple helix (Rout, Mondal, Chakraborty, & Islam, 2008).

3.2. Inhibitory effects of AMP40N and AMP40S on BGC-823 cell proliferation

In this study, we have attempted to evaluate the growth inhibition of AMP40N and AMP40S on human gastric carcinoma cells BGC-823 by MTT assay. As shown in Fig. 6, the two polysaccharides exhibited a dose-dependent activity within the concentration range of 25–400 μg/mL. In particular, AMP40S presented a significantly high inhibitory rate of 85.94% at the concentration 400 μg/mL after 72 h incubation. It was also observed that the

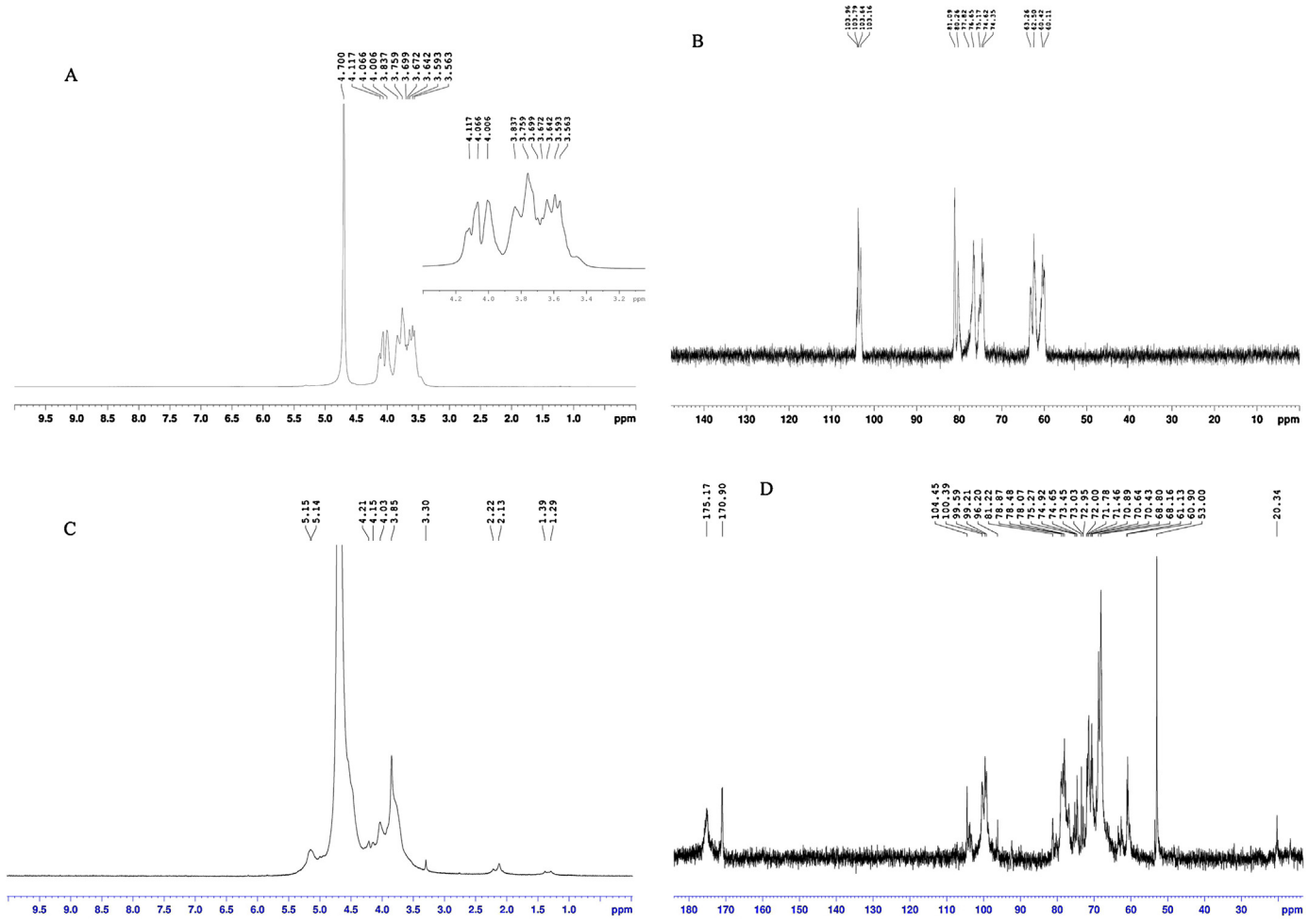

Fig. 5. ^{1}H NMR spectra for AMP40N (A) and AMP40S (C) and ^{13}C NMR spectra for AMP40N (B) and AMP40S (B), respectively.

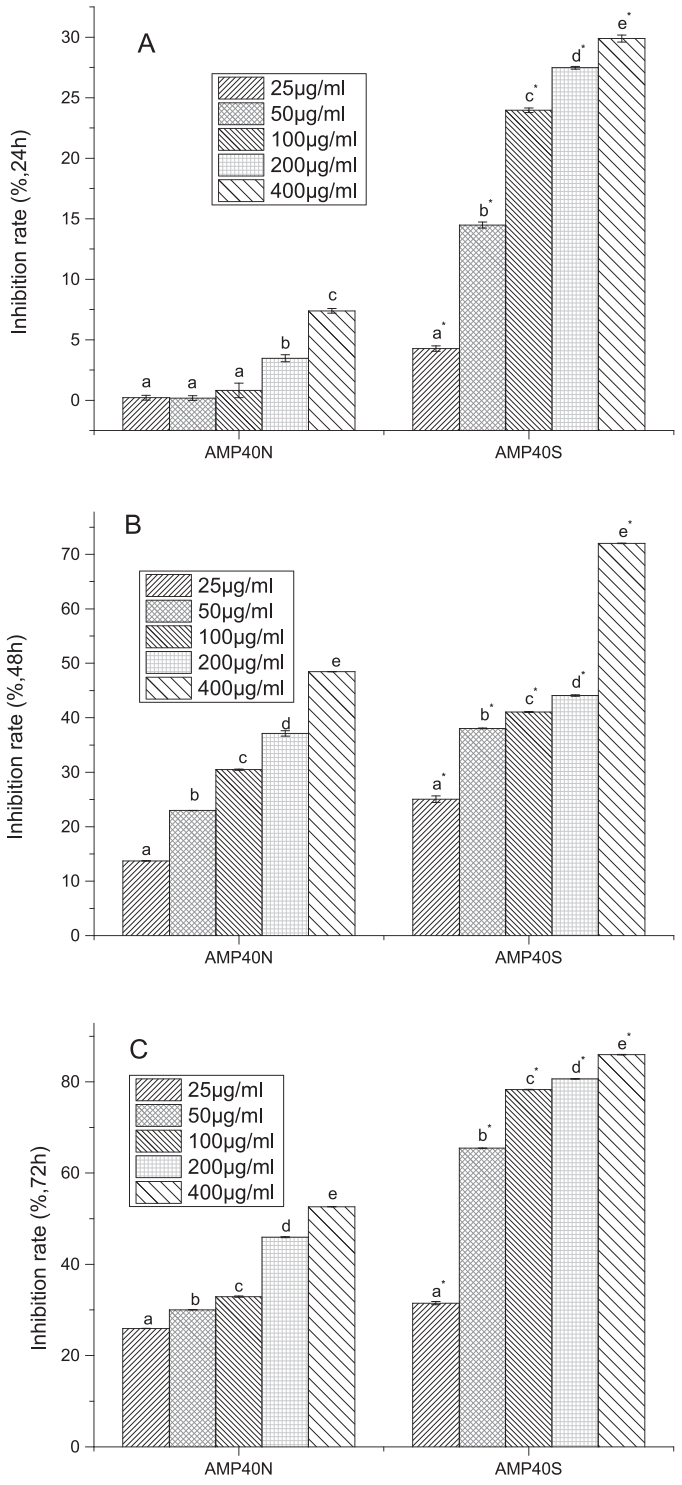

Fig. 6. Inhibition of AMP40N and AMP40-S on the growth of human gastric cancer BGC-823 cells at 24 h (A), 48 h (B) and 72 h (C) treatment. Data are means ± SD of triplicates. Different alphabets (a–e, a*–e*) denote significant difference ($P < 0.05$).

degree of inhibition closely correlated with exposure time at a given concentration. Furthermore, we found that AMP40S exhibited significantly higher anti-tumor activity than AMP40N. The difference of anti-tumor activity for AMP40S and AMP40N might be due to their differences in monosaccharide composition, molecular weight, content of uronic acid and structure. In the monosaccharide composition, AMP40S was more complex than that of AMP40N. Compared with AMP40N, AMP40S had a higher molecular weight. In addition, AMP40S represented relatively higher content of uronic acid than AMP40N. Accordingly, AMP40S exhibited stronger inhibitory effect than AMP40N. The results demonstrate that the molecular weight, chemical property, monosaccharide composition and linkage type of polysaccharide play important roles in the anti-tumor activity of polysaccharides (Huang et al., 2007; Zhang, Gu, et al., 2010).

4. Conclusions

According to the results stated above, it could be concluded that the water extracted AMP40 predominantly contained a neutral polysaccharide (AMP40N) and an acidic polysaccharide (AMP40S). AMP40N and AMP40S were quite different in their contents of uronic acid, molecular weight, monosaccharide composition and type of glycosidic linkage. Both exhibited strong anti-tumor potential according to the assay of inhibitory activity on BGC-823 cells *in vitro*, in particular, AMP40S presented a significantly higher inhibition rate than AMP40N. The difference might be due to their differences in molecular weight, uronic acid content, monosaccharide composition and type of glycosidic linkage. Further works on the structure and biological activity are in progress.

Acknowledgment

This work was supported by a grant-in-aid for scientific research from the National Natural Science Foundation of China (31201454), the Fundamental Research Funds for the Central Universities (KYZ201218), a Project Funded by the Priority Academic Program Development of Jiangsu Higher Education Institutions (PAPD) and by Natural Science Foundation of Jiangsu Province (BK20141269).

References

Alsop, R. M., & Vlachogiannis, G. J. (1982). Determination of the molecular-weight of clinical dextran by gel-permeation chromatography on TSK-Pw-type columns. *Journal of Chromatography A*, *246*, 227–240.

Bai, L., Zhu, L. Y., Yang, B. S., Shi, L. J., Liu, Y., Jiang, A. M., et al. (2012). Antitumor and immunomodulating activity of a polysaccharide from *Sophora flavescens* Ait. *International Journal of Biological Macromolecules*, *51*, 705–709.

Blumenkrantz, N., & Asboe-Hansen, G. (1973). New method for quantitative determination of uronic acids. *Analytical Biochemistry*, *54*, 484–489.

Bradford, M. M. (1976). A rapid and sensitive method for the quantitation of microgram quantities of protein utilizing the principle of protein–dye binding. *Analytical Biochemistry*, *72*, 248–254.

Brasch, D. J., Chang, H. M., Chuah, C. T., & Melton, L. D. (1981). The galactan sulfate from the edible, red alga *Porphyran columbina*. *Carbohydrate Research*, *97*, 113–125.

Cai, W., Xie, L., Chen, Y., & Zhang, H. (2013). Purification, characterization and anticoagulant activity of the polysaccharides from green tea. *Carbohydrate Polymers*, *92*, 1086–1090.

Ciucanu, I., & Kerek, F. (1984). A simple and rapid method for the permethylation of carbohydrates. *Carbohydrate Research*, *131*, 209–217.

Dodgson, K. S., & Price, R. G. (1962). A note on the determination of the ester sulfate content of sulfate polysaccharides. *Biochemical Journal*, *84*, 106–110.

Dubois, M., Gilles, K. A., Hamilton, J. K., Rebers, P. A., & Smith, F. (1956). Colorimetric method for determination of sugars and related substances. *Analytical Chemistry*, *28*, 350–356.

Kumar, G. C., Joo, H. S., Choi, J. W., Koo, Y. M., & Chang, C. S. (2004). Purification and characterization of an extracellular polysaccharide from haloalkalophilic *Bacillus* sp I-450. *Enzyme and Microbial Technology*, *34*, 673–681.

Huang, Q., Jin, Y., Zhang, L., Cheung, P. C. K., & Kennedy, J. F. (2007). Structure, molecular size and antitumor activities of polysaccharides from *Poria cocos* mycelia produced in fermenter. *Carbohydrate Polymers*, *70*, 324–333.

Kuroda, M., Mimaki, Y., Kameyama, A., Sashida, Y., & Nikaido, T. (1995). Steroidal saponins from *Allium chinense* and their inhibitory activities on cyclic AMP phosphodiesterase and Na^+/K^+ ATPase. *Phytochemistry*, *40*, 1071–1076.

Li, J., Fan, L., & Ding, S. (2011). Isolation, purification and structure of a new water-soluble polysaccharide from *Zizyphus jujuba cv. Jinsixiaozao*. *Carbohydrate Polymers*, *83*, 477–482.

Lu, X., Mo, X., Guo, H., & Zhang, Y. (2012). Sulfation modification and anticoagulant activity of the polysaccharides obtained from persimmon (*Diospyros kaki* L.) fruits. *International Journal of Biological Macromolecules*, *51*, 1189–1195.

Mosmann, T. (1983). Rapid colorimetric assay for cellular growth and survival: Application to proliferation and cytotoxicity assays. *Journal of Immunological Methods*, *65*, 55–63.

Ogawa, K., Wanatabe, T., Tsurugi, J., & Ono, S. (1972). Conformational behavior of a gel-forming (1→3)-β-glucan in alkaline solution. *Carbohydrate Research*, *23*, 399–405.

Peng, J. P., Wang, X., & Yao, X. S. (1993). Study on two new furostanol glycosides from *Allium macrostemon* Bunge. *Acta Pharmaceutica Sinica*, *28*, 526–531.

Peng, J. P., Yao, X. S., Tezuka, Y., & Kikuchi, T. (1996). Furostanol glycosides from bulbs of *Allium chinense*. *Phytochemistry*, *41*, 283–285.

Qiao, D., Liu, J., Ke, C., Sun, Y., Ye, H., & Zeng, X. (2010). Structural characterization of polysaccharides from *Hyriopsis cumingii*. *Carbohydrate Polymers*, *82*, 1184–1190.

Rout, D., Mondal, S., Chakraborty, I., & Islam, S. S. (2008). The structure and conformation of a water-insoluble (1→3)-,(1→6)-β-D-glucan from the fruiting bodies of *Pleurotus florida*. *Carbohydrate Research*, *343*, 982–987.

Sun, L., Wang, L., & Zhou, Y. (2012). Immunomodulation and antitumor activities of different-molecular-weight polysaccharides from *Porphyridium cruentum*. *Carbohydrate Polymers*, *87*, 1206–1210.

Tian, L., Zhao, Y., Guo, C., & Yang, X. (2011). A comparative study on the antioxidant activities of an acidic polysaccharide and various solvent extracts derived from herbal *Houttuynia cordata*. *Carbohydrate Polymers*, *83*, 537–544.

Wang, X. M., Sun, R. G., Zhang, J., Chen, Y. Y., & Liu, N. N. (2012). Structure and antioxidant activity of polysaccharide POJ-U1a extracted by ultrasound from *Ophiopogon japonicus*. *Fitoterapia*, *83*, 1576–1584.

Wang, Z. M., Peng, X. A., Lee, K. L. D., Tang, J. C. O., Cheung, P. C. K., & Wu, J. Y. (2011). Structural characterisation and immunomodulatory property of an acidic polysaccharide from mycelial culture of *Cordyceps sinensis* fungus Cs-HK1. *Food Chemistry*, *125*, 637–643.

Wong, K. H., Lai, C. K. M., & Cheung, P. C. K. (2011). Immunomodulatory activities of mushroom sclerotial polysaccharides. *Food Hydrocolloids*, *25*(2), 150–158.

Xie, G., Schepetkin, I. A., & Quinn, M. T. (2007). Immunomodulatory activity of acidic polysaccharides isolated from *Tanacetum vulgare* L. *International Immunopharmacology*, *7*, 1639–1650.

Xie, W. D., Zhang, Y., Wang, N. L., Zhou, H., Du, L. J., Ma, X. H., et al. (2008). Novel effects of macrostemonoside A, a compound from *Allium macrostemon* Bung, on hyperglycemia, hyperlipidemia, and visceral obesity in high-fat diet-fed C57BL/6 mice. *European Journal of Pharmacology*, *599*, 159–165.

Xin, T., Zhang, F., Jiang, Q., Chen, C., Huang, D., Lv, Y., et al. (2012). Purification and antitumor activity of two acidic polysaccharides from the roots of *Polygala tenuifolia*. *Carbohydrate Polymers*, *90*, 1671–1676.

Zha, X. Q., Luo, J. P., Luo, S. Z., & Jiang, S. T. (2007). Structure identification of a new immunostimulating polysaccharide from the stems of *Dendrobium huoshanense*. *Carbohydrate Polymers*, *69*, 86–93.

Zhang, H., Li, J., Xia, J., & Lin, S. (2013). Antioxidant activity and physicochemical properties of an acidic polysaccharide from *Morinda officinalis*. *International Journal of Biological Macromolecules*, *58*, 7–12.

Zhang, S., He, B., Ge, J., Li, H., Luo, X., Zhang, H., et al. (2010). Extraction, chemical analysis of *Angelica sinensis* polysaccharides and antioxidant activity of the polysaccharides in ischemia-reperfusion rats. *International Journal of Biological Macromolecules*, *47*, 546–550.

Zhang, Y., Gu, M., Wang, K. P., Chen, Z. X., Dai, L. Q., Liu, J. Y., et al. (2010). Structure, chain conformation and antitumor activity of a novel polysaccharide from *Lentinus edodes*. *Fitoterapia*, *81*, 1163–1170.

Zhang, Z., Wang, F., Wang, M., Ma, L., & Zeng, X. (2012). Extraction optimisation and antioxidant activities *in vitro* of polysaccharides from *Allium macrostemon* Bunge. *International Journal of Food Science and Technology*, *47*, 723–730.

Zhu, B. W., Li, D. M., Zhou, D. Y., Han, S., Yang, J. F., Li, T., et al. (2011). Structural analysis and CCK-releasing activity of a sulphated polysaccharide from abalone (*Haliotis Discus Hannai* Ino) viscera. *Food Chemistry*, *125*, 1273–1278.